

# Automated multi-target tracking with kinematic and non-kinematic information

S.H. Bae<sup>1</sup> D.Y. Kim<sup>1</sup> J.H. Yoon<sup>1</sup> V. Shin<sup>2</sup> K.-J. Yoon<sup>1</sup>

<sup>1</sup>School of Information and Communications, Gwangju Institute of Science and Technology, 261 Cheomdan-Gwagiro, Buk-Gu, Gwangju 500-712, South Korea

<sup>2</sup>Department of Information and Statistics, Gyeongsang National University, 501 Jinjudaero, Jinju, Gyeongsangnam-do 660-701, South Korea  
E-mail: kjyoon@gist.ac.kr

**Abstract:** The authors address an automated multi-target tracking (MTT) problem. In particular, our study is focused on robust data association considering an additional feature and the reliable track management by avoiding track duplications. As the additional feature, the amplitude information is combined with position measurements to improve the performance of the data association so as to effectively distinguish target-originated measurements from clutters. Because of its form of signal-to-noise ratio (SNR), which is often fluctuated according to targets' aspect and effective radar cross section, the usage of the amplitude information is not straightforward. To reduce the certain level of uncertainty of the SNR, the authors propose the SNR estimation algorithm. Moreover, the authors avoid the track duplication problem to achieve the reliability of track maintenance. Specifically, the authors solve the problem by exploiting well-known mean shift algorithm to merge duplications into appropriate clusters. Simulation results demonstrate the effectiveness and high estimation accuracy of the proposed MTT filter compared to existing methods.

## 1 Introduction

The aim of this paper is to design an automatic multi-target tracking (MTT) system using sensor measurements under cluttered environment. The crucial tasks of the automatic MTT system are composed of an initiation of tentative tracks, an estimation of target states and a track management based on measurements with some prior knowledge: dynamic and measurement model, target detection probability, clutter distribution and so on.

In the cluttered environment, sensor receives mixed observations reflected from targets and clutters [1]. Generally, to distinguish target observations from clutters, thresholding algorithm such as constant false alarm detection [2] is exploited and then the refined observations which contain the kinematic information, for example range, bearing and velocity of targets, are used as inputs of the tracker. However, the clutters could not be completely removed in the detection process because of the difficulty of finding the optimal threshold. Moreover, observations from clutters would dominate the target observations which lead to false positives. Hence, to achieve more accurate automatic MTT with uncertain kinematic measurements, the most important problem is how to correctly identify the target-originated measurement and exclude the clutter. This is known as a data association problem.

A vast amount of work has been published on MTT filters related to the development of data association algorithm with kinematic information [1, 3–8]. Joint probability data

association (JPDA) [1] and multiple hypothesis tracking (MHT) filters [3] are the most well known of them. However, the filters have limitations when targets are closely spaced or heavy clutters are distributed in the vicinity of targets. In these cases, the reason is because the kinematic information is not sufficient to correctly assign measurements to the corresponding tracks. To this extend, some improvements can be possible if we additionally consider another type of feature that is distinctive in such situations.

Practical applications of radar, sonar and acoustics provide kinematic properties as well as non-kinematic information, for example, amplitude. The main focus of this paper is to utilise the non-kinematic information with kinematic information to improve the data association. However, we should be careful in dealing with the amplitude information because it is not straightforward to obtain the explicit model which describes the direct relationship between the target kinematic and the amplitude information. This implies that exploiting amplitude information to estimate target state can be challenging. Instead of using the amplitude in the target state estimate, it is rather effective to utilise the common assumption that the amplitude information of a target is stronger than that of clutters to the data association process.

Based on this finding, the paper [9] demonstrated that the amplitude information can be exploited in the data association process with the kinematic one. Thus, we adopt the amplitude information to enhance the performance of the data association rather than the estimation of target state with complex modelling.

The non-kinematic information can be incorporated in the data association process with a likelihood ratio between target and clutter amplitude likelihood functions. These likelihood functions are based on probability density functions (pdfs) of target and clutter amplitudes. Assume that the received signal is affected by Rayleigh fading, pdf of the amplitude becomes Rayleigh distribution according to the target signal-to-noise ratio (SNR) [9] which should be given a priori. This assumption is known to be appropriate for scan-to-scan slow fluctuation (Swerling I) and pulse-to-pulse fast fluctuation (Swerling II) models [10, 11], and they are mostly used in the probabilistically modelling of returns from aircrafts.

However, most of the developed filters using the non-kinematic information have a strict assumption that the target SNR is known without any filtering which is not realistic [9, 12, 13]. Generally, it is not easy to determine the target SNR in advance since it is often randomly fluctuated according to target's aspect or effective radar cross section [10, 14]. To overcome this limitation, we propose a novel algorithm to estimate the unknown SNRs of multi-target based on the sequential Monte Carlo (SMC) method [15–17]. Once estimation of targets' SNRs is available, we can employ it with the kinematic information to enhance the performance of data association in MTT.

In the automatic MTT, another important task is a reliable track management to prevent track duplications. Track duplications usually occur in the track initiation process especially when several consecutive detections appear near the true track. In particular, the duplications are resulted when automatically initialising tentative tracks [18] without initial true target information, for example target's location and appearance time. In this case, the duplication brings about significant degradation of MTT performance in terms of accuracy and time complexity. To alleviate the duplications, we classify the duplicated tracks using the mean-shift [19]. Then, we determine a tentative track of each group and its tracking components using our own rule which will be specifically discussed in Section 4.4.

Based on robust data association with additional non-kinematic information and reliable track management, we implement the automated MTT system. The proposed system shows better performance especially for a non-linear model in heavy cluttered environment and the situation where the target number is frequently changing. Through a challenging MTT example, the proposed MTT filter is compared and analysed with a different set-up.

The remainder of the paper is organised as follows: Section 2 presents the dynamic system, the non-linear measurement model and some notations. In Section 3, we give preliminaries for probabilistic amplitude modelling with known SNR. Subsequently, the SNR estimation algorithm via SMC method is demonstrated.

Our overall automated MTT system is designed including track management in Section 4. To evaluate the efficiency and robustness of proposed system, a numerical example is tested in Section 5. Finally, conclusions are drawn in Section 6.

## 2 Problem statement

A linear discrete-time dynamic system model of multiple targets is represented as follows

$$x_k^t = F_k x_{k-1}^t + v_k^t, \quad k = 1, 2, \dots \quad (1)$$

where  $x_k^t = [x_{1,k}^t \ x_{2,k}^t \ x_{3,k}^t \ x_{4,k}^t]^T \in \mathbb{R}^4$  denote  $t$ th target kinematic states at time instant  $k$   $x_{1,k}^t$  and  $x_{3,k}^t$  represent  $x$  and  $y$  coordinate position, and  $x_{2,k}^t$  and  $x_{4,k}^t$  describe velocities along with  $x$  and  $y$  coordinate, respectively.  $F_k$  is a transition matrix for the constant velocity model and  $v_k \sim N(0, Q_k^t)$  is normally distributed acceleration noise of zero mean and white Gaussian. We assume that the number of target is unknown since the target quantity may change according to appearance of new targets and disappearance of existing targets. The initial target states  $x_0^t$  are assumed to be Gaussian  $x_0^t \sim N(m_0^t, P_0^t)$ ,  $m_0 = E(x_0)$  and  $P_0 = \text{cov}\{x_0^t, x_0^t\}$ .

When a target is assumed to appear, then a track  $\tau$  is initiated to sequentially estimate the target state. Here, the number of tracks is not perfectly matched with the number of true targets in practical situations because of the false tracks initiated by clutters.

At time instant  $k$ , a set of measurements containing kinematic and non-kinematic components is received. The set includes returns from both targets and clutters, but their origins are not known. Notations for measurements (i.e. target and clutters) are given as follows:

- $Z^k$  – the sequence of kinematic (range and bearing) and non-kinematic (amplitude) measurement sets up to time  $k$ , that is,  $Z^k = [Z^{p,k} \ Z^{a,k}]^T$ ,  $Z^{p,k} = [Z^{r,k} \ Z^{\theta,k}]^T$ ;
- $Z^{r,k}$ ,  $Z^{\theta,k}$  and  $Z^{a,k}$  – respectively, the sequences of range, bearing and amplitude measurement sets up to time  $k$ , that is;  $Z^{r,k} = \{Z_1^r, \dots, Z_k^r\}$ ,  $Z^{\theta,k} = \{Z_1^\theta, \dots, Z_k^\theta\}$  and  $Z^{a,k} = \{Z_1^a, \dots, Z_k^a\}$ ;
- $Z_k^r$ ,  $Z_k^\theta$  and  $Z_k^a$  – respectively, a set of range, bearing and amplitude measurements at time instant  $k$ , that is,  $Z_k^r = \{z_1^r, \dots, z_{m_k}^r\}$ ,  $Z_k^\theta = \{z_1^\theta, \dots, z_{m_k}^\theta\}$  and  $Z_k^a = \{z_1^a, \dots, z_{m_k}^a\}$ ,  $i = 1, \dots, m_k$ , where  $m_k$  is the number of detected measurements at time  $k$ ;
- $Z_k^\tau$  – a set of measurements in a validation gate of track  $\tau$  at time instant  $k$ ,  $Z_k^\tau = \{z_{1,k}^\tau, \dots, z_{m_k}^\tau\}$ ,  $i = 1, \dots, m_k^\tau$ ;
- $z_{i,k}^\tau$  – the  $i$ th gated measurement of track  $\tau$  with range, bearing and amplitude components, that is,  $z_{i,k}^\tau = [z_{i,k}^{r,\tau} \ z_{i,k}^{\theta,\tau} \ z_{i,k}^{a,\tau}]^T \in \mathbb{R}^3$ .

Note that  $z_{i,k}^\tau$  is the  $i$ th measurement of  $Z_k^\tau$  which is located within the validation gate of track  $\tau$ . We assume that each target detection is obtained according to the known target detection probability  $P_D^\tau$ , and the detection falls inside the gate with gate probability  $P_G^\tau$ . We adopt the same gating technique already utilised in probabilistic data association filter (PDAF) [1] to reduce the complexity of the track-to-measurement assignment.

Using a gating technique, a set of validated measurement is represented as

$$Z_k^\tau = \{z_{i,k}^\tau : (v_{i,k}^\tau)^T (S_k^\tau)^{-1} (v_{i,k}^\tau) \leq \gamma\} = \{z_{1,k}^\tau, \dots, z_{m_k}^\tau\}, \quad i = 1, \dots, m_k^\tau \quad (2)$$

where  $\gamma$  is the gate threshold and  $m_k^\tau$  is the number of measurements in the gate of track  $\tau$  at time instant  $k$ .  $v_{i,k}^\tau = z_{i,k}^\tau - \bar{z}_k^\tau$  is a zero-mean Gaussian residual with covariance  $S_k^\tau$  (17). A predicted measurement  $\bar{z}_k^\tau$  is calculated by  $\bar{z}_k^\tau = h_k(\hat{x}_{k|k-1})$ , where  $\hat{x}_{k|k-1} = F_k \hat{x}_{k-1|k-1}$  is the predicted estimates.

We consider that a target-originated measurement is described by a non-linear measurement model that includes

the range, the bearing, and the amplitude information as

$$z_{i,k} = h_k(x_k^t) + w_k$$

$$= \begin{bmatrix} \sqrt{(x_{1,k}^t)^2 + (x_{3,k}^t)^2} \\ \tan^{-1}\left(\frac{x_{3,k}^t}{x_{1,k}^t}\right) \\ a_k^t \end{bmatrix} + \begin{bmatrix} w_{r,k} \\ w_{\theta,k} \\ 0 \end{bmatrix}, \quad k = 1, 2, \dots \quad (3)$$

where the range noise  $w_{r,k} \sim N(0, \sigma_r^2)$  and the bearing noise  $w_{\theta,k} \sim N(0, \sigma_\theta^2)$  are uncorrelated Gaussian noise sequences. We assume that the  $i$ th amplitude measurement  $z_{i,k}^a$  is independent from  $i$ th kinematic measurements  $z_{i,k}^p = [z_{i,k}^r, z_{i,k}^\theta]^T$ , which implies that

$$p(z_{i,k}^p, z_{i,k}^a | Z^k) = p(z_{i,k}^p | Z^{p,k}) p(z_{i,k}^a | Z^{a,k}), \quad Z^k = [Z^{p,k} \ Z^{a,k}]^T \quad (4)$$

In the next section, the amplitude measurement from target or clutter is discussed.

### 3 Probabilistic amplitude information modelling

In this section, we explain how the amplitude information can be described with a probabilistic model by relating with the target SNR which is usually assumed to be known. To apply the amplitude information in a more practical case, we propose an SNR estimation algorithm.

#### 3.1 Amplitude likelihood function

Let us assume that the amplitude  $a$  is the output of a bandpass matched filter followed by an envelope detector. The propagation and attenuation of the amplitude  $a$  are modelled with Rayleigh distribution as given in [9]. Without loss of generality, the time index  $k$  is omitted. Note that the target SNR is defined as a power ratio which is an expected power of received signal over a normalised background noise power. We denote  $d$  as the target SNR and assume that clutter SNR is equal to 0 dB. It means that the expected power of the clutter is considered as the power of back ground noise. In this paper, we assume that the amplitude  $a$  is treated as the realisation of Rayleigh distributed random value given the target SNR  $d$ .

Let us consider the amplitude  $a$  exceeds a detection threshold DT;  $a \geq \text{DT}$ . If the amplitude  $a$  is originated from a target, then the pdf of the  $a$  is given as

$$p_1^{\text{DT}}(a, d) = \frac{1}{P_D} p_1(a, d) = \frac{a}{1+d} \exp\left(\frac{\text{DT}^2 - a^2}{2(1+d)}\right),$$

$$p_1(a, d) = p_1^{\text{DT}=0}(a, d) \quad (5)$$

$$P_D = \int_{\text{DT}}^{\infty} p_1(a) da = \exp\left(\frac{-\text{DT}^2}{2(1+d)}\right)$$

Otherwise, originated from clutters, whose pdf of the

$a$  is given as

$$p_0^{\text{DT}}(a) = \frac{1}{P_{\text{FA}}} p_0(a) = a \exp\left(\frac{\text{DT}^2 - a^2}{2}\right),$$

$$p_0(a) = p_0^{\text{DT}=0}(a), \quad P_{\text{FA}} = \int_{\text{DT}}^{\infty} p_0(a) da = \exp\left(-\frac{\text{DT}^2}{2}\right) \quad (6)$$

where  $P_D$  and  $P_{\text{FA}}$  are target and clutter detection probabilities. When the target SNR  $d$  is given, amplitude likelihood functions of the target and the clutter are calculated as follows

$$g_a^{\text{DT}}(a|d) = p_1^{\text{DT}}(a, d) \quad (7)$$

$$c_a^{\text{DT}} = p_0^{\text{DT}}(a) \quad (8)$$

Once  $g_a^{\text{DT}}(a|d)$  and  $c_a^{\text{DT}}$  are provided, we can exploit the amplitude information to enhance the track-to-measurement association (see Section 4.2 for details).

#### 3.2 Unknown SNR estimation

As mentioned in the Introduction, the assumption of knowing the target SNR is not feasible in practical cases because the SNR is fluctuated according to properties of the target. To exploit the amplitude without the assumption, we propose to estimate an unknown target SNR based on the SMC approach [15–17]. For track  $\tau$ , a set of amplitude measurements passed through the gating (2) and the amplitude thresholding, that is,  $a_{i,k} \geq \text{DT}$ , becomes

$$Z_k^a = \{a_{1,k}, \dots, a_{i,k}\}, \quad i = 1, \dots, m_k^\tau \quad (9)$$

where  $a_{i,k}$  is the  $i$ th amplitude measurement in the gate whose pdf follows Rayleigh distribution with the unknown SNR  $d_{i,k}^\tau$ .

We assume that the possible target SNR  $d_{i,k}^\tau$  lies in a potential SNR interval, that is,  $d_{i,k}^\tau \in [d_1, d_2]$ .  $d_1$  and  $d_2$  are minimum and maximum values of the specified boundary. We consider the pdf of  $d_{i,k}^\tau$  to be uniform within certain boundary  $[d_1, d_2]$ . Then, the unknown target SNR  $d_{i,k}^\tau$  can be written as

$$p(d_{i,k}^\tau) = \begin{cases} \frac{1}{d_2 - d_1}, & d_1 \leq d_{i,k}^\tau \leq d_2, \quad i = 1, \dots, m_k^\tau \\ 0, & \text{otherwise} \end{cases} \quad (10)$$

The unknown SNR  $d_{i,k}^\tau$  can be estimated with  $N$  samples, that is,  $d_k^1, \dots, d_k^N$ , and corresponding weight  $w_k^l$ . We have

$$\hat{d}_{i,k}^\tau = \sum_{l=1}^S w_k^l d_k^l, \quad i = 1, \dots, m_k^\tau \quad (11)$$

where  $d_k^l$  is  $l$ th sample distributed according to  $p(d_{i,k}^\tau)$  (10), and  $S$  is total number of samples. The weight  $w_k^l$  is proportional to amplitude likelihood function  $p_1^{\text{DT}}(a_{i,k}, d_k^l)$ , that is

$$w_k^l \propto p_1^{\text{DT}}(a_{i,k}, d_k^l), \quad i = 1, \dots, m_k^\tau, \quad l = 1, \dots, S \quad (12)$$

Now, we can utilise the estimated SNR  $\hat{d}_{i,k}^\tau$  to compute a

target amplitude likelihood function  $g_a^T(a|d)$  (7) without the knowledge of the target SNR as a given parameter.

Fig. 1 demonstrates the estimation result for five targets for different SNRs (10, 15, 20, 25 and 30 dB) using the proposed algorithm. The boundary  $[d_1, d_2]$  is taken with between 0 and 30 dB. One hundred samples are randomly generated within the boundary. We observe that each estimated value asymptotically converges to true SNRs. Furthermore, we calculate the root mean square errors (RMSEs) for each true SNR (dB)  $d_k$  and its corresponding estimated SNR (dB)  $\hat{d}_k$  based on 500 Monte Carlo simulations

$$\text{RMSE (dB)} = \sqrt{\frac{1}{500} \sum_{s=1}^{500} \|\hat{d}_{s,k} - d_{s,k}\|^2}$$

We show that the errors are rapidly converged for all cases. Therefore these results verify that our SNR estimation algorithm can effectively estimate the unknown SNR.

In the proposed automated MTT algorithm, we utilise the estimated SNR to enhance the data association between the targets and the clutters as described in the following section.

#### 4 Automated MTT with amplitude information

In this section, our automated MTT system is proposed including the track initialisation, the filtering, the data association and the track management. The automatic track initialisation can be achieved using the two-step initialisation (TSI) method. The converted measurement Kalman filter (CMKF) is introduced as a non-linear tracking filter. As a

main contribution, we present an improved data association algorithm with the amplitude information based on the estimated SNR. Then, we show that each track can be managed according to the track existence probability. To deal with tracker duplication in MTT, we propose a novel track merging algorithm using the mean shift. Following subsections subsequently describe each component of the proposed system and the overall algorithms are summarised for the brief review of our automated MTT system.

##### 4.1 Unbiased converted measurement

In this paper, the CMKF [20] is exploited to estimate states of targets in the non-linear measurement system. One main reason of this choice is to account for the practical implementation by reducing the computation complexity. We briefly introduce the CMKF equations as follows. For simplicity, the track index  $\tau$  and measurement index  $i$  are omitted in this section.

CMKF uses a polar-to-Cartesian transformation to convert the polar coordinate measurements  $z_k^p = [z_k^r \ z_k^\theta]^T$  into the Cartesian coordinate  $z_k^c = [P_k^x \ P_k^y]^T$

$$P_k^x = r_k \cos \theta_k; \quad P_k^y = r_k \sin \theta_k, \quad r_k = z_k^r \quad \text{and} \quad \theta_k = z_k^\theta \quad (13)$$

The error covariance for the unbiased converted measurements is used as given in [20] (see (14)).

where  $\sigma_r^2$  is the range error variance and  $\lambda_\theta$  is the compensation factor;  $\lambda_\theta = \exp(-\sigma_\theta^2/2)$ .

Based on the polar-to-Cartesian transformation, the non-linear measurement model (3) can be rewritten with the

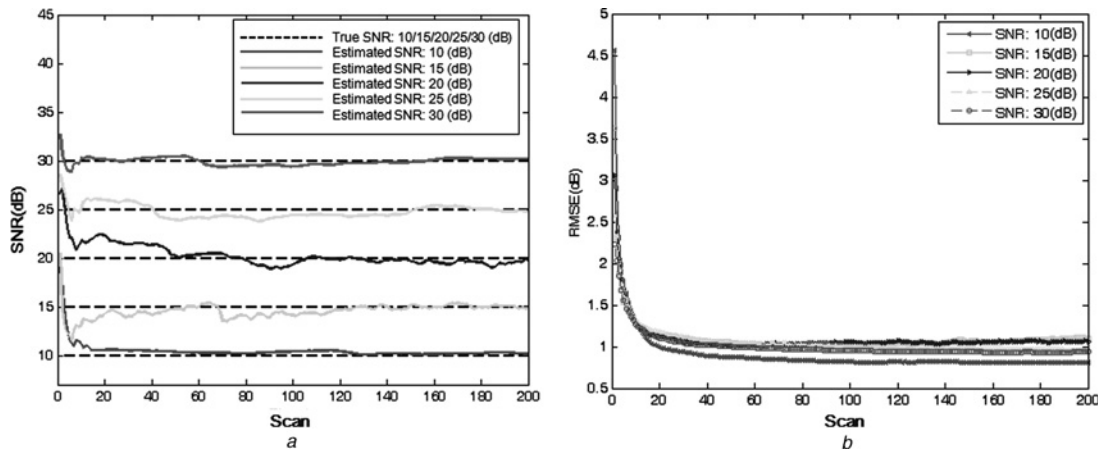


Fig. 1 Estimation result for five targets

a True and estimated SNR values with (11). The dotted lines represent true SNRs for 10, 15, 20, 25 and 30 dB. The lines show estimated results for each SNR  
b RMSEs between true and estimated SNRs are displayed with different types of markers

$$R_k^c = \begin{pmatrix} R_k^{11} & R_k^{12} \\ R_k^{21} & R_k^{22} \end{pmatrix}, \quad \begin{cases} R_k^{11} = (\lambda_\theta^{-2} - 2)r_k^2 \cos^2(\theta_k) + 0.5(r_k^2 + \sigma_r^2)(1 + \lambda_\theta^4 \cos(2\theta_k)) \\ R_k^{12} = (\lambda_\theta^{-2} - 2)r_k^2 \cos(\theta_k) \sin(\theta_k) + 0.5(r_k^2 + \sigma_r^2)\lambda_\theta^4 \sin(2\theta_k) \\ R_k^{21} = R_k^{12} \\ R_k^{22} = (\lambda_\theta^{-2} - 2)r_k^2 \sin^2(\theta_k) + 0.5(r_k^2 + \sigma_r^2)(1 - \lambda_\theta^4 \cos(2\theta_k)) \end{cases} \quad (14)$$

unbiased converted measurement model as

$$z_k = \begin{bmatrix} z_k^c \\ a_k^t \end{bmatrix} = \begin{bmatrix} H_k x_k^t \\ a_k^t \end{bmatrix} + \begin{bmatrix} w_{x,k} \\ w_{y,k} \\ 0 \end{bmatrix} \quad (15)$$

$$k = \begin{bmatrix} 1 & 0 & 0 & 0 \\ 0 & 0 & 1 & 0 \end{bmatrix}, \quad H_k = 1, 2, \dots$$

where  $w_{x,k} \sim N(0, R_k^{11})$  and  $w_{y,k} \sim N(0, R_k^{22})$  and are Gaussian distributed position noises along with  $x$  and  $y$  coordinates, and  $R_k^{11}$  and  $R_k^{22}$  are calculated by (14).

Kalman prediction and update step at time instant  $k$  are described in (16) and (17)

- Prediction step

$$\hat{x}_{k|k-1} = F_k \hat{x}_{k-1|k-1}$$

$$P_{k|k-1} = F_k P_{k-1|k-1} F_k^T + Q_k \quad (16)$$

- Update step

$$S_k = H_k P_{k|k-1} H_k^T + R_k^c$$

$$K_k = P_{k|k-1} H_k^T S_k^{-1} \quad (17)$$

$$x_{k|k} = \hat{x}_{k|k-1} + K_k (\lambda_\theta^{-1} z_k^c - H_k \hat{x}_{k|k-1}), \quad z_k^c = [P_k^x \ P_k^y]^T$$

$$P_{k|k} = (I - K_k H_k) P_{k|k-1}$$

## 4.2 Data association with amplitude information

To implement the data association in our automated MTT, we adopt the linear multi-target integrated probabilistic data association (LMIPDA) approach [21]. The main reason is that the LMIPDA simply calculates the data association probability to avoid the exponentially growing combinatorial. This filter exploits a modified scatter measurement density by considering possibilities that the measurements may be originated from other targets or clutters. As a result, the LMIPDA has reasonable computational complexity by ignoring the joint track-to-measurement assignment of JPDAF [1] or MHT [3]. For more details on the LMIPDA refer to [21].

Based on the LMIPDA framework, we propose to include the amplitude information to improve the data association by incorporating the kinematic and amplitude likelihood functions. A new algorithm is called LMIPDA-Amplitude Information (LMIPDA-AI). For the unknown SNR case, the amplitude likelihood function can be effectively calculated using our SNR estimation algorithm. The proposed LMIPDA-AI could provide the high accuracy and the robustness especially when targets are closely spaced or enormous clutters exist.

To derive the LMIPDA-AI, let us denote some notations for random events of track  $\tau$  and measurement  $i$ .

- $\chi_k^\tau$ : The event that track  $\tau$  exists at time instant  $k$ .
- $\chi_{i,k}^\tau$ : The event that the  $i$ th measurement  $z_{i,k}^\tau$  is associated with track  $\tau$ .
- $\chi_{0,k}^\tau$ : The event that none of the gated measurements are not associated with track  $\tau$ .

In addition, clutter measurements are modelled with properties as follows:

1. The number of clutter measurement is according to a homogeneous Poisson process with a known spatial clutter density  $\rho^c$ .
2. The clutter is uniformly distributed in the validation region  $V$ .

For each gated measurement  $z_{i,k}^\tau$ , we define the clutter density  $\rho_{i,k}$  including a kinematic component and the amplitude component as

$$\rho_{i,k} \equiv \rho(z_{i,k}^\tau) = \rho(z_{i,k}^{c,\tau}) \rho(z_{i,k}^{a,\tau}) = \rho_{i,k}^c \cdot c_k^{\text{DT}}(a_{i,k}), \quad i = 1, \dots, m_k^\tau \quad (18)$$

where the kinematic clutter density  $\rho_{i,k}^c = \rho^c$  is a known constant by the homogeneous assumption (1) and  $c_k^{\text{DT}}(a_{i,k})$  is (8).

Given the converted measurement sequence sets  $Z^k = [Z^{c,k} \ Z^{a,k}]^T$ , the likelihood of the  $z_{i,k}^\tau = [z_{i,k}^{c,\tau} \ z_{i,k}^{a,\tau}]^T$  given track  $\tau$  can be defined based on independent assumption (4)

$$\Lambda_i^\tau \equiv P(z_{i,k}^\tau | \chi_k^\tau, Z^{k-1}) = P(z_{i,k}^{c,\tau} | \chi_k^\tau, Z^{c,k-1}) P(z_{i,k}^{a,\tau} | \chi_k^\tau, Z^{a,k-1})$$

$$= \Lambda_{i,k}^{c,\tau} \Lambda_{i,k}^{a,\tau}, \quad i = 1, \dots, m_k^\tau \quad (19)$$

where the kinematic likelihood function  $\Lambda_{i,k}^{c,\tau}$  and the non-kinematic likelihood  $\Lambda_{i,k}^{a,\tau}$  become

$$\Lambda_{i,k}^{c,\tau} = N(v_{i,k}^\tau, S_k^\tau) = \exp\left(-\frac{1}{2} (v_{i,k}^\tau)^T (S_k^\tau)^{-1} v_{i,k}^\tau\right),$$

$$v_{i,k}^\tau = z_{i,k}^{c,\tau} - \bar{z}_k^{c,\tau}, \quad \bar{z}_k^{c,\tau} = H_k \hat{x}_{k|k-1}$$

$$\Lambda_{i,k}^{a,\tau} = g_a^{\text{DT}}(a_{i,k}^\tau | \hat{a}_{i,k}^\tau), \quad i = 1, \dots, m_k^\tau \quad (20)$$

Here residual  $v_{i,k}^\tau$  and its covariance  $S_k^\tau$  are yielded with (16) and (17). Estimated target SNR  $\hat{a}_{i,k}^\tau$  is given by (11).

In LMIPDA-AI, a priori data association probabilities  $P_{i,k}^\tau$  means that  $z_{i,k}^\tau$  is associated with track  $\tau$  and approximately yielded with the amplitude information as follows

$$P_{i,k}^\tau \equiv P(\chi_{i,k}^\tau, \chi_k^\tau | Z^{k-1}) \simeq P_D^\tau P_G^\tau P(\chi_k^\tau | Z^{k-1}) \frac{\Lambda_{i,k}^\tau}{\rho_{i,k}} / \sum_{i=1}^{m_k^\tau} \frac{\Lambda_{i,k}^\tau}{\rho_{i,k}},$$

$$\Lambda_{i,k}^\tau = \Lambda_{i,k}^{c,\tau} \Lambda_{i,k}^{a,\tau}, \quad \rho_{i,k} = \rho_{i,k}^c \cdot c_k^{\text{DT}}(a_{i,k}) \quad (21)$$

where  $P_D^\tau$  and  $P_G^\tau$  are target detection and gate probabilities.  $P(\chi_k^\tau | Z^{k-1})$  is the propagation of target existence probability  $P(\chi_{k-1}^\tau | Z^{k-1})$  and represented with Markov chain one model as

$$P(\chi_k^\tau | Z^{k-1}) = \Delta_{11} P(\chi_{k-1}^\tau | Z^{k-1}) + \Delta_{21} (1 - P(\chi_{k-1}^\tau | Z^{k-1})) \quad (22)$$

with transition probability

$$\Delta_{11} \equiv P(\chi_k^\tau | \chi_{k-1}^\tau) \text{ and } \Delta_{21} \equiv P(\chi_k^\tau | \tilde{\chi}_{k-1}^\tau)$$

where  $\tilde{\chi}_k^\tau$  denotes non-existence of the track at time  $k$ .

Using (19) and (21), the posterior probabilities of target existence can be derived as follows

$$P(\chi_k^\tau | Z^k) = \frac{(1 - \Psi_k^\tau) \cdot P(\chi_k^\tau | Z^{k-1})}{1 - \Psi_k^\tau \cdot P(\chi_k^\tau | Z^{k-1})},$$

$$\Psi_k^\tau = P_D^\tau P_G^\tau \left( 1 - \sum_{i=1}^{m_k^\tau} \frac{\Lambda_{i,k}^\tau}{\Phi_{i,k}^\tau} \right), \quad \Lambda_{i,k}^\tau = \Lambda_{i,k}^{c,\tau} \Lambda_{i,k}^{a,\tau} \quad (23)$$

where  $\Phi_{i,k}^\tau$  is a priori scatter measurement density of measurement  $z_{i,k}^\tau$  using (18), (19) and (22) becomes

$$\Phi_{i,k}^\tau = \underbrace{\rho_{i,k}}_{\text{clutter}} + \underbrace{\sum_{\substack{\sigma=1 \\ \sigma \neq \tau}}^{M_k} \Lambda_{i,k}^\sigma \frac{P_{i,k}^\sigma}{1 - P_{i,k}^\sigma}}_{\text{other target}},$$

$$\rho_{i,k} = \rho_{i,k}^c \cdot c_k^{\text{DT}}(a_{i,k}), \quad \Lambda_{i,k}^\sigma = \Lambda_{i,k}^{c,\sigma} \Lambda_{i,k}^{a,\sigma}, \quad i = 1, \dots, m_k^\tau \quad (24)$$

Here  $\Phi_{i,k}^\tau$  is the probability that the measurement  $z_{i,k}^\tau$  is originated from the scatterer, that is, clutter or other target: the first term and second term separately represent that the probability  $z_{i,k}^\tau$  originated from a clutter and other target.  $M_k$  is the total number of track at time instant  $k$ .

Posteriori data association probabilities in LMIPDA-AI can be derived as follows

$$\left( \beta_{0,k}^\tau = \frac{P(\chi_{0,k}^\tau, \chi_k^\tau | Z^k, M_k)}{P(\chi_k^\tau | Z^k, M_k)} = \frac{1 - P_D^\tau P_G^\tau}{1 - \Psi_k^\tau}, \right.$$

$$\left. \Psi_k^\tau = P_D^\tau P_G^\tau \left( 1 - \sum_{i=1}^{m_k^\tau} \frac{\Lambda_{i,k}^\tau}{\Phi_{i,k}^\tau} \right) \right) \quad (25)$$

$$\beta_{i,k}^\tau = \frac{P(\chi_{i,k}^\tau, \chi_k^\tau | Z^k, M_k)}{P(\chi_k^\tau | Z^k, M_k)} = \frac{P_D^\tau P_G^\tau \Lambda_{i,k}^\tau}{1 - \Psi_k^\tau \Phi_{i,k}^\tau},$$

$$i = 1, \dots, m_k^\tau \quad (26)$$

For each track  $\tau$ , posteriori state estimate  $\hat{x}_k^\tau$  and covariance  $P_{k|k}^\tau$  are calculated by combining local estimates  $\hat{x}_{i,k|k}^\tau$  (17) and association probabilities  $\beta_{i,k}^\tau$  (25) and (26)

$$\hat{x}_{k|k}^\tau = \sum_{i=0}^{m_k^\tau} \beta_{i,k}^\tau \hat{x}_{i,k|k}^\tau \quad (27)$$

$$P_{k|k}^\tau = \sum_{i=0}^{m_k^\tau} \beta_{i,k}^\tau [P_{i,k|k}^\tau + (\hat{x}_{i,k|k}^\tau - \hat{x}_{k|k}^\tau)(\hat{x}_{i,k|k}^\tau - \hat{x}_{k|k}^\tau)^T] \quad (28)$$

### 4.3 Track initialisation and management

At time instant  $k$ , tentative tracks are initiated by the previous kinematic measurements  $Z_{k-1}^c$  and the current kinematic measurements  $Z_k^c$  within a rectangle region using the TSI [18]. The region is determined with maximum velocities of the target along the  $x$  and  $y$  coordinates and unbiased

converted covariance  $R_k^c$  (14) as

$$\text{Rectangle region} = \left[ 2 \left( V_{x, \max} T_s + 2\sqrt{R_k^{11}} \right) + \right]$$

$$\times \left[ 2 \left( V_{y, \max} T_s + 2\sqrt{R_k^{22}} \right) \right] \quad (29)$$

Once the tracks are automatically initiated by the TSI, then we could estimate targets' states using CMKF and LMIPDA-AI as previously discussed. Our remaining task to complete the automated MTT system is to make a sophisticated track management algorithm. The desirable track management algorithm should identify true tracks which are followed true targets, and eliminate false tracks not followed. In this paper, we can manage lots of tracks with only considering the track existence probability  $P(\chi_k^\tau | Z^k)$  (23). Specifically, our strategy for the efficient track management is to divide track status into three cases and manage tracks according to their status.

- A track is initialised using TSI with an initial existence probability  $P_1(\chi_0^\tau)$ .
- A track is confirmed when  $P(\chi_k^\tau | Z^k)$  exceeds a confirmation threshold  $\vartheta_c$  and two steps have passed since the track is initialised.
- A track is terminated when  $P(\chi_k^\tau | Z^k)$  falls below a termination threshold  $\vartheta_e$  or predicted states of track locate outside the surveillance area.

### 4.4 Track merging

In the MTT without initial true target information, several confirmed tracks often estimate same targets. Generally, this problem is called track duplication. To circumvent the duplications, we classify tracks into some groups according to their estimated states by exploiting the mean shift [19]. Then, we select the most likely true track in each group. Based on the mean shift, each track is classified around the significant modes.

Given estimated states of tracks  $\hat{x}_{k|k}^\tau$ ,  $\tau = 1, \dots, M_k$ , we can find the modes of estimated states with a multivariate kernel. Let us denote the sequence of successive locations of the kernel by  $\{y_j\}_{j=1,2,\dots}$  and the location are iteratively determined as

$$y_{j+1} = \frac{\sum_{\tau=1}^{M_k} \hat{x}_{k|k}^\tau g\left(\frac{\|y_j - \hat{x}_{k|k}^\tau\|^2}{h}\right)}{\sum_{\tau=1}^{M_k} g\left(\frac{\|y_j - \hat{x}_{k|k}^\tau\|^2}{h}\right)}, \quad j = 1, 2, \dots, \quad (30)$$

where  $y_1$  is the centre of the initial kernel,  $h > 0$  is a bandwidth of kernel and  $g(x)$  is derivative of the Epanechnikov kernel profile  $k_E(x)$ , that is,  $g(x) = -k_E'(x)$

$$k_E(x) = \begin{cases} \frac{1}{2} c_d^{-1} (d+2) (1 - \|x\|^2), & \|x\| \leq 1 \\ 0, & \text{otherwise} \end{cases} \quad (31)$$

where  $d = 4$  is the dimension of target states and  $c_d$  is the volume of the unit four-dimensional sphere.

By the iterative operation (31), each mode can be found when the magnitude of the mean shift vector  $\mathbf{m}_{h,G}(y_j)$

converges to zero.

$$m_{h,c}(y_j) = y_{j+1} - y_j = 0 \quad (32)$$

For  $M_k$  tracks, the clusters  $\{C_q\}_{1,\dots,m_c}$  are determined by  $m_c$  modes (converged points) and bandwidth  $h$ . In this paper, we define a group when Euclidean distance between  $\hat{x}_{k|k}^\tau$  and  $m_c$  is closer to  $4 \times h$ .

Let us denote a tentative true track  $\{q^*\}_{1,\dots,m_c}$  in each cluster  $\{C_q\}_{1,\dots,m_c}$ . Then, components of the track  $q^*$  are determined as described:

- The track states  $\hat{x}_{k|k}^{q^*}$  is the mode of the cluster  $\{C_q\}_{1,\dots,m_c}$ .
- The covariance  $P_{k|k}^{q^*}$  is the  $\min(P_{k|k}^{\{C_q\}})$ .
- The track existence probability  $P(\chi_k^{q^*} | Z^k)$  is the  $\max(P(\chi_k^{\{C_q\}} | Z^k))$ .
- The track  $q^*$  is confirmed if there is a confirmed track of the cluster  $\{C_q\}$ .

In these steps, we note that the total number of tentative true tracks is the same as the number of clusters.

#### 4.5 Summary of the automated MTT

In summary, the automated MTT process is carried out from the following steps:

- Step 1:* The set of polar coordinates (range and bearing)  $Z_k^p = [Z_k^r Z_k^\theta]^T$  is converted into a set of Cartesian coordinates ( $x$  and  $y$  coordinate positions)  $Z_k^c$  using (13), and the set  $Z_k = [Z_k^c Z_k^a]^T$  are updated in our MTT systems.
- Step 2:* Tentative tracks are initiated by TSI as in Section 4.3.
- Step 3:* For each track  $\tau$ , the validated measurements  $Z_k^\tau$  are determined in the  $Z_k$  through the validation gate (2) and the amplitude detection thresholding DT.
- Step 4:* For each track  $\tau$ , prediction step (16) is performed, and target SNR is estimated based on the proposed SNR estimation algorithm as in Section 3.2.
- Step 5:* For each track  $\tau$ , the posterior probability of target existence  $P(\chi_k^\tau | Z^k)$  (23) and posteriori data association probability  $\beta_{i,k}^\tau$  (25) and (26) are calculated with the proposed LMIPDA-AI as in Section 4.2.
- Step 6:* For each track  $\tau$ , posterior state estimates  $\hat{x}_k^\tau$  (27) and covariance  $P_{k|k}^\tau$  (28) are yielded as in Section 4.2.
- Step 7:* Tracks are managed using their existence probability  $P(\chi_k^\tau | Z^k)$  as in Section 4.3.
- Step 8:* Duplicated tracks are integrated by our merging strategy as in Section 4.4.

## 5 Simulation results

In this section, several versions of LMIPDA and LMIPDA-AI have been implemented in an MTT scenario. We examine the performance of the proposed filter (6) by considering different conditions of (known and estimated) SNR. Furthermore, to verify the effectiveness of the amplitude information and the track merging method given in Section 4.4, we test the original LMIPDA with and without two functionalities.

1. LMIPDA [21].
2. LMIPDA with known SNR (LMIPDA-AI).
3. LMIPDA with estimated SNR (LMIPDA-EAI).
4. LMIPDA with track merging (LMIPDA-MG).

5. LMIPDA with known SNR and with track merging (LMIPDA-AI-MG).
6. LMIPDA with estimated SNR and with track merging (LMIPDA-EAI-MG).

where the filters (1) and (4) use only with kinematic information (range and bearing) without amplitude. In known SNR cases (2) and (5), the filters have information about the true SNR of each target.

### 5.1 Ground moving MTT

We generate ten targets, and each target appears and disappears independently. The target dynamic motion is modelled with a ground moving target model.

$$x_k^t = \begin{bmatrix} 1 & T_s & 0 & 0 \\ 0 & 1 & 0 & 0 \\ 0 & 0 & 1 & T_s \\ 0 & 0 & 0 & 1 \end{bmatrix} x_{k-1}^t + \begin{bmatrix} 0 & 0 \\ T_s & 0 \\ 0 & 0 \\ 0 & T_s \end{bmatrix} v_k, \quad t = 1, \dots, 10 \quad (33)$$

where each target state  $x_k^t \in \mathbb{R}^4$  contains two-dimensional positions and velocities along with  $x$  and  $y$  coordinates. Sampling time  $T_s$  equal to 0.5 and  $v_k = [v_{x,k} \ v_{y,k}]^T$  is white Gaussian noise with a diagonal covariance matrix  $Q_k = \text{diag}[1 \ 1]^T$ . The initial states of the ten targets and their surveillance time are listed in Table 1.

At time instant  $k$ , a set of measurements  $Z_k = [Z_k^r \ Z_k^\theta \ Z_k^a]^T$  containing range, bearing and amplitude information disturbed from white Gaussian noise (3) are generated. Noise variances of  $w_{r,k}$  and  $w_{\theta,k}$  are  $\sigma_r^2 = 10$  and  $\sigma_\theta^2 = 2$ , respectively. Target and clutter amplitudes according to Rayleigh distribution (5) and (6) are generated with each target SNR in Table 1 and clutter SNR (0 dB). To show effectiveness of our SNR estimation algorithm, the target SNRs are considered as the unknown constants. In the proposed SMC-based SNR algorithm, we design the proposal density as the uniform distribution given in (10) to draw the samples  $\{d_{i,k}\}_{i=1, \dots, S}$ .

The sensor detection region is determined with a radial distance range [0 m–1000 m] and a angle range [0°–360°]. Within the detection region, clutters are uniformly distributed. The number of the clutters is tuned by the clutter density  $\lambda$  in Table 2. All true target trajectories are generated according to the scenario in Table 1. In Fig. 2,

**Table 1** Initial target states, SNRs and times at which they appear and disappear

| Target | Initial states                   | Target SNR, dB | Appearing time | Disappearing time |
|--------|----------------------------------|----------------|----------------|-------------------|
| 1      | $[-300 \ 0.00 \ 200 \ -0.50]^T$  | 15             | 3              | 250               |
| 2      | $[-850 \ 1.50 \ -250 \ -0.10]^T$ | 10             | 30             | 280               |
| 3      | $[-400 \ 1.00 \ -378 \ -0.50]^T$ | 5              | 50             | 180               |
| 4      | $[400 \ -0.15 \ -300 \ -0.05]^T$ | 10             | 100            | 200               |
| 5      | $[125 \ 1.00 \ 100 \ 0.05]^T$    | 20             | 20             | 270               |
| 6      | $[150 \ 0.75 \ -150 \ 0.75]^T$   | 20             | 60             | 280               |
| 7      | $[250 \ 0.00 \ 200 \ 0.50]^T$    | 15             | 120            | 300               |
| 8      | $[500 \ -1.25 \ 600 \ -0.25]^T$  | 5              | 100            | 250               |
| 9      | $[750 \ -1.00 \ -250 \ 0.10]^T$  | 25             | 100            | 250               |
| 10     | $[-200 \ 0.25 \ 500 \ 0.25]^T$   | 5              | 150            | 300               |

**Table 2** Filter parameters

| Parameters   | Description  | Value   |
|--|--|---|
| DT   | Amplitude detection threshold                      | 1   |
| $P_D$  | Target detection probability                       | 0.90  |
| $P_G$  | Gate probability                                   | 0.95  |
| S  | Number of samples for SNR estimation               | 60  |
| $\gamma$   | Gate threshold                                     | 9   |
| $\Delta_{11} = P(\chi_k^T   \chi_{k-1}^T)$                 | Transition probabilities of Markov chain one model | 0.98  |
| $\Delta_{21} = P(\tilde{\chi}_k^T   \tilde{\chi}_{k-1}^T)$ |  | 0.02  |
| $V_{x,max}$  | Maximum velocity of target along x                 | 10 m/s  |
| $V_{y,max}$  | Maximum velocity of target along y                 | 10 m/s  |
| $\lambda$  | Clutter density                                    | $3 \times 10^{-5}$ measurements/scan/m <sup>2</sup> |
|  |  | $5 \times 10^{-5}$ measurements/scan/m <sup>2</sup> |
|  |  | $10^{-4}$ measurements/scan/m <sup>2</sup>          |
| $h$  | Bandwidth of kernel                                | 1   |
| $d_1$  | Minimum value in SNR boundary                      | 1 (0 dB)  |
| $d_2$  | Maximum value in SNR boundary                      | 1000 (30 dB)  |
| $P_1(\chi_0^T)$  | Initial target existence probability               | 0.8   |
| $\vartheta_c$  | Confirmation threshold                             | 0.8   |
| $\vartheta_e$  | Termination threshold                              | 0.1   |

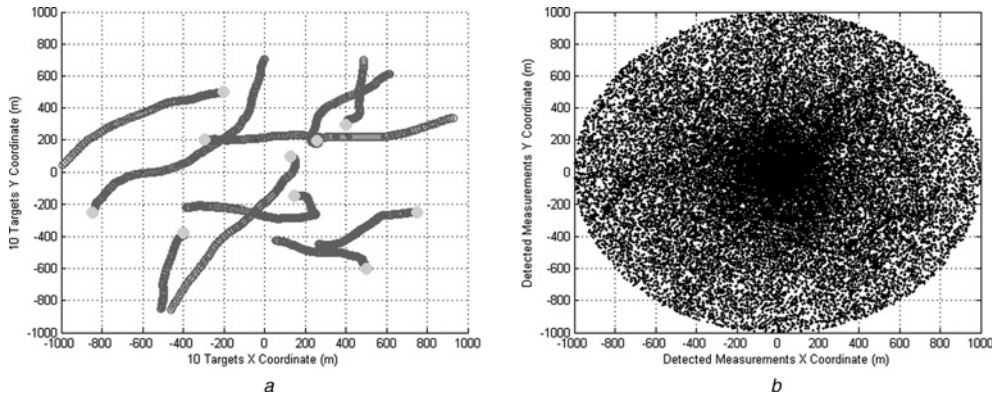


**Fig. 2** True trajectories of ten targets and all detected measurements

a True trajectories of the ten targets over 300 scans: line-trajectories, circle-initial target positions  
 b Detected measurement positions from the ten targets and clutters over 300 scans at  $\lambda = 10^{-4}$ . Around 100 clutters appear per each scan

true trajectories of ten targets and all detected measurements are depicted over 300 scans. In this scenario, all filters (1)–(6) struggle to solve the MTT problem with the same filter parameters in Table 2.

**5.2 Optimal subpattern assignment (OSPA) metric**

The performance of the filters (1)–(6) is examined with the OSPA metric [22] as a performance measure. Given two finite sets, that is, a true set and an estimated set of multi-target state, we can evaluate the performance of MTT in terms of OSPA metric which simultaneously represents ‘localisation errors’ and ‘cardinality errors’. The localisation errors mean the accuracy between true states and estimated states of multi-target. The cardinality errors demonstrate how the number of trackers matches with the true number of objects. The ‘total error’, OSPA distance, is the sum of ‘total localisation errors’ and ‘total cardinality errors’ and represents the overall quality of the multi-target tracker. Let us  $X = \{x_1, \dots, x_m\}$  and  $Y = \{y_1, \dots, y_n\}$  denote the true set and the estimated set of target states. The OSPA

distance  $\bar{d}_p^{(c)}$  is defined as

$$\bar{d}_p^{(c)}(X, Y) \equiv \left( \frac{1}{n} \left( \min_{\pi \in \Pi_n} \sum_{j=1}^m d^{(c)}(x_i, y_{\pi(j)})^p + c^p(n - m) \right) \right)^{1/p} \tag{34}$$

if  $m \leq n$ , and  $\bar{d}_p^{(c)}(X, Y) \equiv \bar{d}_p^{(c)}(Y, X)$  if  $m > n$ ; and  $\bar{d}_p^{(c)}(X, Y) = \bar{d}_p^{(c)}(Y, X) = 0$  if  $m = n = 0$ . Here,  $\bar{d}_p^{(c)}(x, y) \equiv \min(c, ||x - y||)$  is the distance  $d$ . The cut-off parameter  $c$  determines the relative weighing of the penalties assigned to cardinality and localisation errors. The order parameter  $p$  determines the sensitivity of the metric to outliers. We select  $c = 100$  and  $p = 1$ .

**5.3 Comparison results with different MTT filters**

Based on the 500 Monte Carlo simulations, the time-averaging results of OSPA metric between the true sets and the estimated set of targets state for the filters (1)–(6) are given in Table 3. Also, we provide computation costs of filters (1)–(6) in

**Table 3** Time-averaging results of OSPA metric between the sets of true state and the sets of estimated states and computation time for filters (1)–(4)

| Filters clutter density $\lambda$ , measurements/scan/m <sup>2</sup> | LMIPDA  | LMIPDA-AI | LMIPDA-EAI | LMIPDA-MG | LMIPDA-AI-MG | LMIPDA-EAI-MG |
|--|---------|-----------|------------|-----------|--------------|---------------|
| (A) OSPA distance  |         |           |            |           |              |               |
| $3 \times 10^{-5}$   | 43.4968 | 40.0861   | 41.5285    | 31.5362   | 28.5781      | 29.2299       |
| $5 \times 10^{-5}$   | 54.1097 | 47.3180   | 48.7565    | 39.5441   | 30.2316      | 31.4228       |
| $1 \times 10^{-4}$   | 62.5559 | 50.6407   | 51.7760    | 58.7436   | 32.9661      | 34.7473       |
| (B) OSPA localisation distance                                       |         |           |            |           |              |               |
| $3 \times 10^{-5}$   | 17.3358 | 15.5584   | 16.0428    | 9.2184    | 7.4999       | 7.5188        |
| $5 \times 10^{-5}$   | 22.0095 | 18.7623   | 19.7203    | 13.5399   | 7.8196       | 7.9632        |
| $1 \times 10^{-4}$   | 26.9685 | 20.7944   | 21.8048    | 23.9849   | 9.2191       | 9.9692        |
| (C) OSPA cardinality distance  |         |           |            |           |              |               |
| $3 \times 10^{-5}$   | 26.1610 | 25.1308   | 25.4857    | 22.3178   | 21.0781      | 21.7111       |
| $5 \times 10^{-5}$   | 32.1002 | 28.5557   | 29.0592    | 26.0042   | 22.4119      | 23.4597       |
| $1 \times 10^{-4}$   | 35.5874 | 29.8463   | 29.9712    | 34.7586   | 23.7471      | 24.7781       |
| (D) Computation time (s/scan)  |         |           |            |           |              |               |
| $3 \times 10^{-5}$   | 0.0319  | 0.0254    | 0.0273     | 0.0298    | 0.0225       | 0.0253        |
| $5 \times 10^{-5}$   | 0.0637  | 0.0501    | 0.0572     | 0.0737    | 0.0542       | 0.0601        |
| $1 \times 10^{-4}$   | 0.2339  | 0.1595    | 0.1865     | 0.2956    | 0.2956       | 0.3010        |

**Table 3.** In the detection region, approximately 30, 50 and 100 clusters are generated for different  $\lambda$  values,  $3 \times 10^{-5}$ ,  $5 \times 10^{-5}$ , and  $10^{-4}$ , respectively.

In **Table 3**, we confirm that the performance of filter can be considerably improved by exploiting amplitude information by comparing (1) with (2) and (3). For all OSPA errors (A)–(C), (2) and (3) show better accuracy than the filter (1) without the amplitude. In particular, the differences between the performance of filters (1)–(3) are clearly distinguishable in high clutter density  $\lambda = 10^{-4}$ . This result can be understood that the filters (2) and (3) with the amplitude information can effectively distinguish unknown origin of measurement in the heavy cluttered environment. Surprisingly, the performance difference between the filter (2) and (3) are negligible. From this evaluation, the proposed SNR estimation algorithm effectively estimates target SNR and significantly increases the performance of the data association in MTT.

Additionally, it is evident that our merging method can solve track duplication problem by comparing the filters (1)–(3) with the filters (4)–(6). As expected, the cardinality errors are dramatically reduced in the filters (4)–(6) by incorporating our merging method.

The computation costs of the filters (1)–(4) are evaluated in **Table 3** (D). Based on the comparison between (1) and (2) with filters (3), we find that our SNR estimation algorithm can effectively estimate target SNRs with reasonable computation costs. Moreover, the results demonstrate that the filter (6) exploiting proposed SNR estimation and merging algorithm represents almost the same computation time as the other filters (1)–(5). One possible explanation is that our merging method could eliminate a lot of the duplicated tracks in automated MTT.

In **Fig. 3**, the OSPA distance error is plotted for different clutter densities over time. We obtain the similar comparison results as in **Table 3**. The OSPA distance error of the filters (1) and (4) without amplitude information is much higher than that of other filters at  $\lambda = 10^{-4}$ . During the time of target appearance or disappearance, we observe that the distance errors are slightly increased because of the target cardinality variation. For instance, this phenomenon is distinguishable at scan 100 when three targets have appeared. However, the distance error is quickly reduced by the initiation of new tracks.

Summarising the simulation results described in **Table 3** and **Fig. 3**, we can present following evaluation in terms of

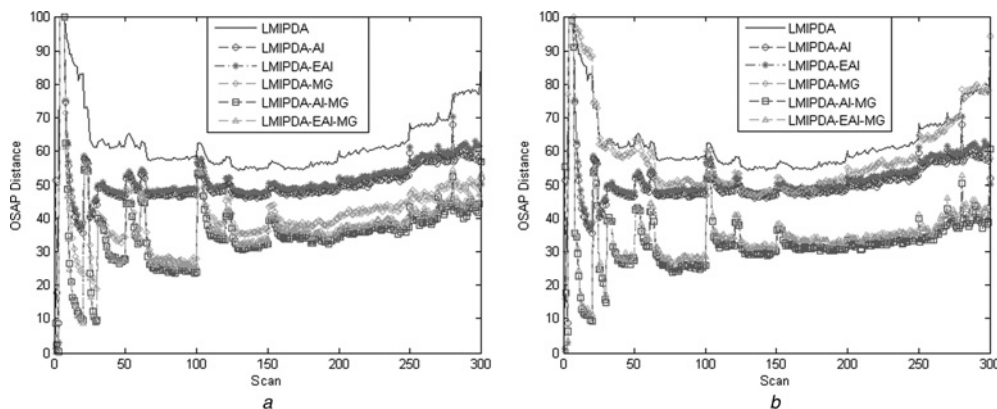


**Fig. 3** Comparison results of the filters (1)–(6) in terms of OSPA distances over 300 scans

a Clutter density  $\lambda = 5 \times 10^{-5}$

b Clutter density  $\lambda = 10^{-4}$

OSPA metric

$$\begin{aligned} \text{LMIPDA} &> \text{LMIPDA-AI} = \text{LMIPDA-EAI} \\ &> \text{LMIPDA-MG} > \text{LMIPDA-AI-MG} \\ &= \text{LMIPDA-EAI-MG} \end{aligned}$$

## 6 Conclusions

In this paper, we propose the automated MTT system which is composed of the track initialisation, tracking, the data association and the maintenance. To exploit the amplitude information in practical cases, we propose the SNR estimation algorithm based on the SMC method. We propose the LMIPDA-AI to effectively combine the amplitude information with the kinematic information based on our estimation algorithm. For the efficient track management, we exploit the track existence probability. To prevent degradation of performance incurred by the track duplication, a novel track merging method is additionally suggested.

The performance evaluation of our proposal was demonstrated using an MTT scenario in terms of OSPA metric. As shown in the experiment results, our automated MTT system can effectively estimate states of multi-target for non-linear system in cluttered environment with reasonable computation costs.

## 7 Acknowledgment

This work was supported by the Basic Research Project through a grant provided by Gwangju Institute of Science and Technology (GIST).

## 8 References

- 1 Bar-Shalom, Y., Li, X.R.: 'Multitarget – multisensor tracking: principles and techniques' (YBS Publishing, 1995)
- 2 Gini, F., Greco, M.V., Farina, A.: 'Clairvoyant and adaptive signal detection in non-Gaussian clutter: a data-dependent threshold interpretation', *IEEE Trans. Signal Process.*, 1999, **47**, (6), pp. 1522–1531
- 3 Blackman, S.: 'Multiple hypothesis tracking for multi target tracking', *IEEE Trans. Aerosp. Electron. Syst.*, 2004, **19**, (1), pp. 5–18
- 4 Hue, C., Le Cadre, J.-P., Perez, P.: 'Sequential Monte Carlo methods for multiple target tracking and data fusion', *IEEE Trans. Signal Process.*, 2002, **50**, (2), pp. 309–325
- 5 Musicki, D., Evans, R.: 'Joint integrated probabilistic data association-JIPDA', *IEEE Trans. Aerosp. Electron. Syst.*, 2004, **40**, (3), pp. 1093–1099
- 6 Yoon, J., Kim, D., Bae, S., Shin, V.: 'Joint initialization and tracking of multiple moving objects using Doppler information', *IEEE Trans. Signal Process.*, 2011, **59**, (7), pp. 3447–3452
- 7 Wang, X., Musicki, D., Ellem, R., Fletcher, F.: 'Efficient and enhanced multi-target tracking with Doppler measurements', *IEEE Trans. Aerosp. Electron. Syst.*, 2009, **45**, (4), pp. 1400–1417
- 8 Tobias, M., Lanterman, A.D.: 'Probability hypothesis density-based multitarget tracking with bistatic range and Doppler observations', *IEE Proc. Radar Sonar Navig.*, 2005, **152**, (3), pp. 195–205
- 9 Lerro, D., Bar-Shalom, Y.: 'Automated tracking with target amplitude information'. American Control Conf., 2009, pp. 2875–2880
- 10 Slocumb, B.J., Klusman, M.E.: 'A multiple model SNR/ RCS likelihood ratio score for radar-based feature-aid tracking'. Proc. SPIE. Signal and Data Processing of Small Targets 2005, San Diego, CA, USA, 2 August 2005, vol. 5913
- 11 Swerling, P.: 'Probability of detection for fluctuating target', *IRE Trans. Inf. Theory*, 1960, **58**, (1), pp. 26–37
- 12 Song, T.L., Kim, D.S.: 'Highest probability data association for active sonar tracking'. Proc. Ninth Int. Conf. on Information Fusion, Florence, 10–13 July 2006
- 13 Ehrman, L.M., Blair, W.D.: 'Comparison of methods for using target amplitude to improve measurement-to-track association in multi-target tracking'. Proc. Ninth Int. Conf. on Information Fusion, Florence, Italy, 10–13 July 2006
- 14 Clark, D., Ristic, B., Vo, B.N., Vo, B.T.: 'Bayesian multi-object filtering with amplitude feature likelihood for unknown object SNR', *IEEE Trans. Signal Process.*, 2010, **58**, (1), pp. 26–37
- 15 Ristic, B., Arulampalam, S., Gordon, N.: 'Beyond the Kalman filter: particle filter for tracking application' (Artech House, 2004)
- 16 Arulampalam, M.S., Maskell, S., Gordon, N., Clapp, T.: 'A tutorial on particle filters for non-linear/non-Gaussian Bayesian filtering', *IEEE Trans. Signal Process.*, 2002, **50**, (2), pp. 174–188
- 17 Simon, D.: 'Optimal state estimation: Kalman, H infinity, and nonlinear approach' (Wiley-Interscience, 2006)
- 18 Bar-Shalom, Y., Chang, K.C., Blom, H.A.P.: 'Automatic track formation in clutter with recursive algorithm'. Proc. 28th IEEE Conf. on Decision and Control, Tampa, Florida, 13–15 December 1989, pp. 1402–1408
- 19 Comanciu, D., Meer, P.: 'Mean shift: a robust approach toward feature space analysis', *IEEE Trans. Pattern Anal. Mach. Intell.*, 2002, **24**, (5), pp. 603–619
- 20 Mo, L., Song, X., Zhou, Y., Sun, Z.K., Bar-Shalom, Y.: 'Unbiased converted measurements for tracking', *IEEE Trans. Aerosp. Electron. Syst.*, 2009, **34**, (3), pp. 1023–1027
- 21 Musicki, D., Evans, R.: 'Multi-target tracking in clutter without measurement assignment', *IEEE Trans. Aerosp. Electron. Syst.*, 2008, **44**, (3), pp. 877–896
- 22 Schuhmacher, D., Vo, B.-T., Vo, B.-N.: 'A consistent metric for performance evaluation of multi-object filters', *IEEE Trans. Signal Process.*, 2008, **56**, (8), pp. 3447–3457